Mem. S.A.It. Vol. 85, 684

Memorie della

New constraints on the formation and settling of dust in the atmospheres of young M and L dwarfs

E. Manjavacas[1], M. Bonnefoy[1,2], J. E. Schlieder[1], F. Allard[3], P. Rojo[4], B. Goldman[1], G. Chauvin[2], D. Homeier[3], N. Lodieu[5,6], and T. Henning[1]

[1] Max Planck Institute für Astronomie, Königstuhl, 17. D-69117 Heidelberg, Germany
e-mail: manjavacas@mpia.de
[2] UJF-Grenoble1/CNRS-INSU,Institut de Planétologie et d'Astrophysique de Grenoble (IPAG) UMR5274, Grenoble 38041, France
[3] CRAL-ENS, 46, Allée d'Italie , 69364 Lyon Cedex 07, France
[4] Departamento de Astronomia, Universidad de Chile, Casilla 36-D, Santiago, Chile
[5] Instituto de Astrofísica de Canarias (IAC), Vía Láctea s/n, E-38206 La Laguna, Tenerife, Spain
[6] Departamento de Astrofísica, Universidad de La Laguna (ULL), E-38205 La Laguna, Tenerife, Spain

Abstract. We obtained medium-resolution ISAAC near-infrared spectra of seven young M9.5-L3 dwarfs classified at optical wavelengths. We compared our targets spectra to those of mature and young BDs, and to young late-type companions to nearby stars with known ages, to identify and study gravity-sensitive features. We computed spectral indices weakly sensitive to the surface gravity to derive near-infrared spectral types. Finally, we found the best fit between each spectrum and synthetic spectra from the BT-Settl 2010 and 2013 atmospheric models. Using the best fit, we derived the atmospheric parameters of the objects and identified which spectral characteristics the models do not reproduce. BT-Settl models fit the spectra and the 1-5 μm spectral energy distribution of the L0-L3 dwarfs for temperatures between 1600-2000 K. But the models fail to reproduce the shape of the H band and the near-infrared slope of some of our targets. This fact, and the best-fit solutions found with super-solar metallicity, are indicative of a lack of dust, in particular at high altitude, in the cloud models.

Key words. stars: -low mass, brown dwarfs, planetary systems – techniques: spectroscopic

1. Introduction

Substellar objects contract and cool down with time (Burrows et al. 1997; Baraffe et al. 1998). Therefore, young objects can have larger radii and higher luminosities than older and more massive objects despite an identical effective temperature. The lower surface gravity of young objects ($g \propto M/R^2$) can be directly accessed by observation and can be used to break the degeneracy. Low surface gravity results in peculiar spectral characteristics such as the triangular H band shape in the near-infrared (Zapatero Osorio et al. 2000; Lucas et al. 2001) and reduced alkali lines in the optical and near-infrared. Atmospheric models allow us to disentangle the effect of varying T_{eff}, log g, and (metallicity) *M/H* on the spectral features. Below $T_{eff} \sim 2600$ K, models predict that clouds of iron and silicate grains begin to form, changing the opacity (Lunine et al. 1986, Tsuji et al. 1996, Burrows & Sharp 1999, Lodders 1999, Marley 2000, Marley & Ackerman 2001, Allard et al. 2001). The formation and the gravitational sedimentation of these dust clouds are influenced by the surface gravity. Dust cloud formation is expected to be more efficient at low gravity because the atmosphere is more extended and the gas is cooler. Low gravity tends to make the convection and the resulting mixing more efficient as well. We present seven medium-resolution spectra of M9.5-L3 dwarfs, classified at optical wavelengths. Our sample is composed of DENIS-P J124514.1-442907 (M9.5), Cha J1305-7739(L0), EROS J0032-4405 (L0γ) and 2MASS J22134491-2136079 (L0γ), 2MASSJ232252.99-615127.5 (L2γ), 2MASS J212650.40-814029.3 (L3γ) and 2MASSJ220813.63+292121.5(L3γ).

2. Observations and data reduction

Our targets were observed with ISAAC mounted on the VLT (UT3). The instrument was operated in low-resolution mode with the 0.3" slit at central wavelengths 1.25, 1.65, and 2.2 μm. This setup provides spectra with resolving powers of ~1700 in J band, 1600 in H band, and 1500 in K band.

Early-type stars were observed soon after the science target at similar airmass to ensure a proper removal of telluric features. Calibrations were obtained during the day following the observations.

Data were reduced using the 6.1.3 version of the ISAAC pipeline (Devillard et al. 1999; Silva & Peron 2004) provided by the *European Southern Observatory*.

Data on the objects and associated telluric standard stars were reduced in a similar way. Telluric standard star spectra were divided by a blackbody with a temperature that corresponded to their spectral type (Theodossiou & Danezis 1991). The He and H lines were interpolated and we obtained the final J, H, and K band spectra of the science targets by dividing them by this transmission.

We flux-calibrated our spectra comparing with 2MASS fluxes coming from the photometry.

3. Empirical analysis

We compare the spectral properties of our sample to those of brown dwarfs and companions found in the literature to confirm features indicative of young age and we also assign near-infrared spectral types for the targets. We select the best fit spectrum using χ^2 minimization as well as visual inspection over all of the wavelengths.

For that purpose, we used spectra of young M- and L-type companions, late-M and early-L brown dwarfs from star forming regions and young nearby associations (Gorlova et al. 2003; Slesnick et al. 2004; Allers et al. 2007; Lodieu et al. 2008; Allers et al. 2009, 2010; Rice et al. 2010; Allers & Liu 2013; Bonnefoy et al. 2014; Manara et al. 2013), young field L dwarfs (Kirkpatrick et al. 2006; Allers & Liu 2013; Liu et al. 2013), and MLT field dwarfs (McLean et al. 2003; Cushing et al. 2005). We also compared our spectra to low resolution spectra (R~120) in the SpeX Prism Spectral Library[1].

To further assess the age, surface gravity, and spectral classes of our targets, we computed spectral indices and alkali lines equivalent widths that quantify the evolution of the main absorption features.

We first used spectral indices measuring the strength of the main water bands. These indices were selected independently by Bonnefoy et al. (2014) and/or Allers & Liu (2013) from Allers et al. (2007) – H_2O, Slesnick et al. (2004) –H_2O-1 and H_2O-2, and McLean et al. (2003) – H_2OD. They are known to show a clear trend with the spectral type,

[1] http://pono.ucsd.edu/~adam/browndwarfs/spexprism/

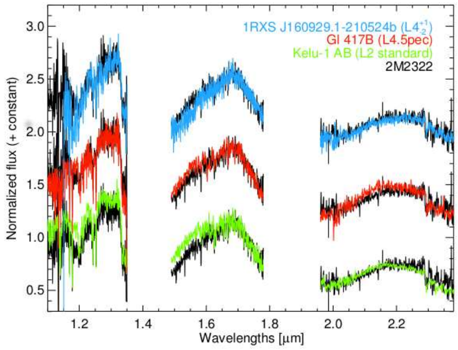

Fig. 1. We show the comparison of the spectrum of 2M2322 to the L2 optical standard, of the young L4.5 binary companion GJ 417B, the planetary mass companion 1RXS J160929.1-210524b

and to be only weakly sensitive to the age or to the gravity class (Cruz et al. 2009). We computed them on the compilation of near-infrared spectra of young M3-M9.5 dwarf members of star forming regions (1-11 Myr) and young nearby associations (age <50 Myr) classified in the optical. We also derived them for young Lγ, Lβ dwarfs, and companion spectra provided by Allers & Liu (2013) and Bonnefoy et al. (2014), and for field dwarfs obtained by McLean et al. (2003) and Cushing et al. (2005). We degrade the resolution of all the spectra to R$\sim$100, which is our lowest resolution. Results are shown in Figure 2. We reajusted a third-order polynomial function on these trends, as in Allers & Liu (2013), and use them to derive spectral type estimates. We calculated the errors in the spectral type as the root mean square (rms). We estimated the final near-infrared spectral types, obtaining the mean of the different estimates from the indices weighted by the associated error, and their errors, as the standard deviation. These estimates are all consistent with the optical spectral types.

The equivalent widths of the gravity-sensitive K I lines at 1.169, 1.177, 1.243, and 1.253 μm of our objects were computed following the method developed by Sembach & Savage (1992). We used the same reference wavelengths for the fit of the pseudocontinuum and for the line as Allers & Liu (2013). In Fig. 3, we show the equivalent widths of these lines as for our targets and reference objects. The trends are similar to those found by Bonnefoy et al. (2014) and Allers & Liu (2013). For all four cases, EROS J0032 has an equivalent widths close to those of field L0 dwarf analogues. The remaining field Lγ dwarfs have lower equivalent widths in some, but not all of the diagrams. The object DENISJ1245 has equivalent widths comparable as late-M dwarf members of the $\sim$8 Myr old TW Hydrae and Upper Scorpius.

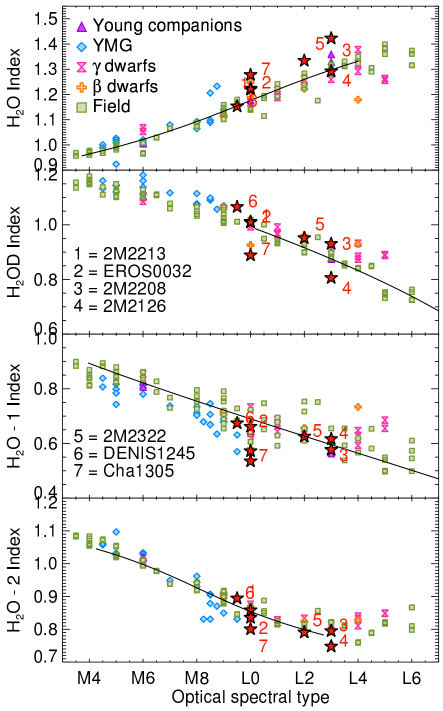

Fig. 2. Spectral indices used for the spectral type estimation of the NIR spectral type. The black lines represent the three degree polynomial fit to the field brown dwarfs.

4. Spectral synthesis

In this section, we compare the near-infrared spectra of our objects to predictions from BT-Settl atmospheric models (Allard et al. 2003,

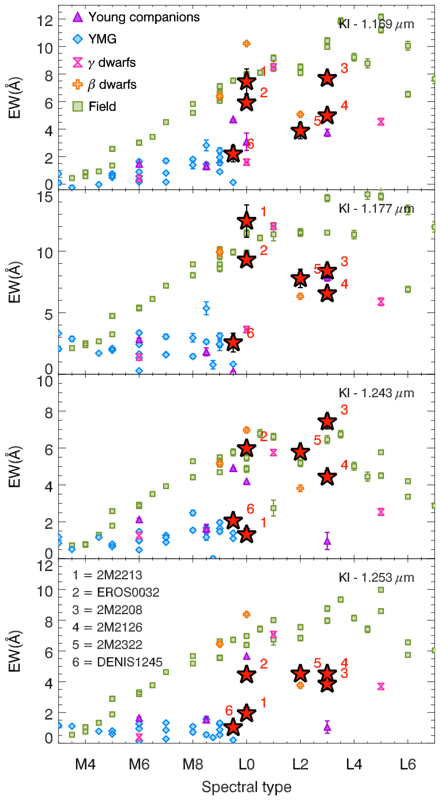

Fig. 3. Equivalent widths for the K I lines at 1.169 μm, 1.177 μm, 1.243 μm, and 1.253 μm for our targets (red stars) and reference objects.

2007, 2011). The models have already been tested on near-infrared spectra of young M5.5-L0 objects by Bonnefoy et al. (2014). We compare the new ISAAC spectra to derive the atmospheric parameters (T_{eff}, log g) of the objects and to reveal nonreproducibilities of the models for later spectral types.

The BT-Settl models account for the formation and gravitational settling of dust grains for T_{eff} below ≈2700 K in the photosphere of the objects, following the approach described in Rossow (1978). The timescales of the main processes (mixing, sedimentation, condensation, coalescence, and coagulation) are compared to determine the density distribution of grains and the average grain size from the innermost to the outermost layers of the cloud.

We selected subgrids of synthetic spectra with 1000 K≤ T_{eff} ≤ 3000 K, 3.0 ≤ log g ≤ 5.5 (≥ 3.5 below 2000 K), and $[M/H]$=0. An alternative subgrid of the BT-Settl 2013 models (1000 K≤ T_{eff} ≤ 3000 K, 3.5 ≤ log g ≤ 5.5) with M/H=+0.5 dex was also used to explore the effect of the metallicity on the determination of log g and T_{eff}. The spacing of the model grid is 100 K and 0.5 dex in log g.

We further test the models by comparing their predictions to the 1-5 μm spectral energy distributions of the objects. We built the spectral energy distributions (SED) of the sources using published photometry from the 2MASS and WISE surveys. We excluded Cha 1305 from this analysis since the SED of this source has a strong excess (Allers et al. 2006). The optical photometry, avaliable for some objects, is not included in the fit because the models are known to be inaccurate at these wavelengths (see Bonnefoy et al. 2014).

The SED fit confirms the effective temperatures found from the near-infrared spectra. Two objects (2M2322, and 2M2126) have best-fit temperatures which disagree with those found from the fit of the BT-Settl 2010 models to the 1.1-2.5 μm spectra. The best fits are found for low surface gravities, therefore further confirming results from the empirical analysis. Nevertheless, the comparison demonstrates that the models do not successfully reproduce the global spectral slope at these wavelengths as well as the pseudocontinuum in the H band.

5. Conclusions

The atmospheric models yield atmospheric parameters that are mostly consistent with our empirical analysis. All of the Lγ objects have surface gravities expected for young objects. The BT-Settl 2013 models converge toward an overall higher surface gravity for EROS J0032.

Surprisingly, all spectra but that of DENIS 1245 are well reproduced by a single BT-Settl 2013 synthetic spectrum with T_{eff}=1800 K, log g = 4.5, and M/H = +0.5. Models at higher metallicity used in this analysis had not been extensively tested. Nonconvergent models can indeed have an

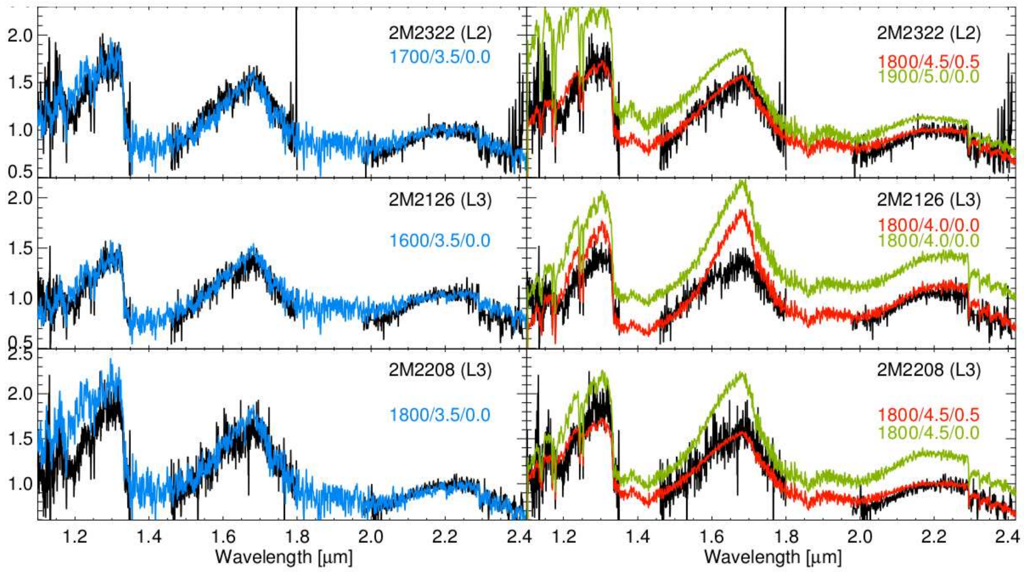

Fig. 4. Visual comparison of the best fit BT-Settl 2010 (left panel, blue) and BT-Settl 2013 (right panel, red) synthetic spectra to some of the ISAAC spectra of young M9.5-L3 dwarfs. Alternative solutions are shown in light green and are shifted by +0.3 to +0.5 flux normalized units for clarity.

anomalous dust content, which can sometimes produce spectra that match the observations well. We found nonetheless that a neighboring spectra with T_{eff} = 1700 K and log g =4.5 is affected by this problem. Therefore, it is possible that our temperature estimate could be biased by 100 K given our inability to check if a convergent model at these T_{eff}'s can provide a better fit. We also verified that the features of the model spectrum at T_{eff} = 1800 K are coherent with those found in model spectra for other neighboring T_{eff} and log g.

The near-infrared spectral slopes, and therefore results from the fits of the ISAAC spectra, are mostly tied to the dust content in the atmosphere. Solutions at high metallicity can then be interpreted as if the 2013 solar metallicity models were not forming enough dust in the atmosphere compared to the 2010 models. This lack of dust could also explain why the models do not reproduce the shape of the pseudocontinuum in the H band well. The mismatch found in the BT-Settl 2010 models is also indicative of a lack of dust grains at high altitude/low optical depths in the cloud model. The problem may be solved with an ongoing revision of the models.

References

Allard, F., et al. 2001, ApJ, 556, 357

Allard, F., Guillot, T., Ludwig, H.-G., et al. 2003, in Brown Dwarfs, Proceedings of the IAU Symp. 211, ed. E. Martín (ASP, San Francisco), 325

Allard, F., Allard, N. F., Homeier, D., et al. 2007, A&A, 474, L21

Allard, F., Homeier, D., & Freytag, B. 2011, in 16th Cambridge Workshop on Cool Stars, Stellar Systems, and the Sun, eds. C. Johns-Krull, M. K. Browning, & A. A. West (ASP, San Francisco), ASP Conf. Ser., 448, 91

Allers, K. N., et al. 2006, ApJ, 644, 364

Allers, K. N., Jaffe, D. T., Luhman, K. L., et al. 2007, ApJ, 657, 511

Allers, K. N., Liu, M. C., Shkolnik, E., et al. 2009, ApJ, 697, 824
Allers, K. N., et al. 2010, ApJ, 715, 561
Allers, K. N., & Liu, M. C. 2013, ApJ, 772, 79
Baraffe, I., et al. 1998, A&A, 337, 403
Bonnefoy, M., Chauvin, G., Lagrange, A.-M., et al. 2014, A&A, 562, AA127
Burrows, A., Marley, M., Hubbard, W. B., et al. 1997, ApJ, 491, 856
Burrows, A. & Sharp, C. M. 1999, ApJ, 512, 843
Cruz, Kirkpatrick & Burgasser, 2009,ApJ, 137, 3345C
Cushing, M. C., Rayner, J. T., & Vacca, W. D. 2005, ApJ, 623, 1115
Devillard, N., Jung, Y., & Cuby, J.-G. 1999, The Messenger, 95, 5
Gorlova, N. I., et al. 2003, ApJ, 593, 1074
Kirkpatrick, J. D., Barman, T. S., Burgasser, A. J., et al. 2006, ApJ, 639, 1120
Liu, M. C., Magnier, E. A., Deacon, N. R., et al. 2013, ApJ, 777, LL20
Lodders, K. 1999, ApJ, 519, 793
Lodieu, N., et al. 2008, MNRAS, 383, 1385
Lucas, P. W., et al. 2001, MNRAS, 326, 695
Lunine, J. I., Hubbard, W. B., & Marley, M. S. 1986, ApJ, 310, 238
Manara, C. F., Testi, L., Rigliaco, E., et al. 2013, A&A, 551, A107
Marley, M. 2000, in From Giant Planets to Cool Stars, eds. C. A. Griffith & M. S. Marley (ASP, San Francisco), ASP Conf. Ser., 212, 152
Marley, M. S. & Ackerman, A. S. 2001, conference proceeding for Planetary Systems in the Universe: Observation, Formation and Evolution, IAU Symposium 202 held 7-10 August 2000, Manchester UK. arXiv:astro-ph/0103269
McLean, I. S., McGovern, M. R., Burgasser, A. J., et al. 2003, ApJ, 596, 561
Rice, E. L., et al. 2010, ApJS, 186, 63
Rossow, W. B. 1978, icarus, 36, 1
Sembach, K. R. & Savage, B. D. 1992, ApJS, 83, 147
Silva, D. R. & Peron, M. 2004, The Messenger, 118, 2
Slesnick, C. L., Hillenbrand, L. A., & Carpenter, J. M. 2004, ApJ, 610, 1045
Theodossiou, E. & Danezis, E. 1991, Ap&SS, 183, 91
Tsuji, T., et al. 1996, A&A, 308, L29
Zapatero Osorio, M. R., Béjar, V. J. S., Martín, E. L., et al. 2000, Science, 290, 103